

DIFFUSIONAL SEPARATION OF CALCIUM ISOTOPES IN CHEMICALLY PECULIAR STELLAR ATMOSPHERES

L. Sapar, A. Sapar, R. Poolamäe and A. Aret
Tartu Observatory, 61602 Tõravere, Estonia; sapar@to.ee

Received: 2014 November 10; accepted: 2014 December 12

Abstract. Diffusional separation of calcium isotopes in the atmospheres of hot chemically peculiar stars is studied. In addition to the usual radiative acceleration effect, the light-induced drift is taken into account. We propose that microturbulence in stable stellar atmospheres is generated by the interaction between plasma particles and radiative flux. Formulae for the microturbulent velocity and microturbulence diffusion coefficient are derived. Data on isotopic and hyperfine splitting of the calcium spectral lines have been collected as an input file. The equilibrium Ca isotope concentrations are found in model computations, iteratively correcting the radiative acceleration values. The general picture of Ca isotope stratification is found to be similar to our previous results obtained for Hg isotopes: dominating overabundance of the heaviest isotope. Diffusional stratification of Ca isotope concentrations in atmospheres of late B and early A spectral types are computed and visualized in figures. The isotope abundances on the inner boundary surface were fixed to be the solar ones. The computed Ca II infrared triplet line profiles are compared with the observed line profiles in a high-dispersion spectrum of HD 175640.

Key words: stars: atmospheres – stars: chemically peculiar – stars: abundances – diffusion – turbulence

1. INTRODUCTION

Peculiarities of spectra of the hot main-sequence chemically peculiar (CP) stars are caused by unusual elemental abundances and isotope ratios in their atmospheres. These stars are traditionally divided into four main classes: metallic-line stars (Am), magnetic peculiar A-stars (Ap), mercury-manganese stars (HgMn) and helium-weak stars (Preston 1974). The HgMn stars have enhanced abundance of many elements, particularly mercury and manganese, while also their peculiar isotopic composition has been established (e.g., Proffitt et al. 1999; Dolk et al. 2003; Castelli & Hubrig 2004a,b; Ryabchikova et al. 2008). These non-variable stars are also characterized by very slow rotational velocities. According to Wolff & Preston (1978) 70% of slowly rotating ($V \leq 5 \text{ km s}^{-1}$) late B-type stars belong to the HgMn type. They have not any regular magnetic field, only weak magnetic fields have been detected (Hubrig et al. 2006).

Generally, peculiar atmospheric elemental composition observed in hot main-sequence CP stars can be explained by the atomic diffusion in radiative field (Michaud 1970). Due to diffusion processes some elements settle down in the atmosphere, while other elements are levitated from interior to the outer layers,

resulting the observed spectral peculiarities. The atmospheres of such peculiar stars must be stable, without convective mixing and meridional circulation caused by stellar rotation.

High-resolution observational spectra make it possible to study isotope anomalies in the atmospheres of HgMn stars. The stellar spectra reveal isotopic shifts (IS) and hyperfine shifts (HFS) of many spectral lines. In many cases the small spectral features are not completely resolved, but their blends are shifting and broadening the lines. In order to study isotope anomalies in astronomical objects and correctly interpret their high resolution spectra, it is necessary in the computations of detailed synthetic spectra of models to take adequately into account the isotopic shifts and hyperfine structure of spectral lines.

However, for many lines the laboratory measurements of the isotopic shifts and the hyperfine shifts are either missing or are of low accuracy, and thus the modeling of the line shifts and profiles has to rely on theoretical values. It is therefore important to undertake further efforts to develop reliable computational methods for both isotopic and hyperfine shifts, which support the detailed analysis of stellar spectra. Stellar spectroscopy needs complete detailed lists of lines and their transition probabilities. Different theoretical approaches can be used for calculations of high-accuracy atomic parameters, for example *ab initio* the computational methods are the many-body perturbation theory, its relativistic version and the multi-configuration Dirac-Hartree-Fock theory, which enable to calculate atomic hyperfine structures, isotopic shifts and electron transition probabilities.

The presence of isotope anomalies in the spectra of CP stars has been established for several elements. Calcium isotope anomaly in the spectra of HgMn stars was detected by Castelli & Hubrig (2004b), studying the infrared triplet (IRT) lines of Ca II in the spectrum of HgMn star HD 175640. They found that spectral lines of Ca II IRT are shifted to the red approximately by 0.2 Å with respect to laboratory wavelengths. The observed redshifts reveal predominance of the heaviest isotope ^{48}Ca compared to other Ca isotopes. Similar shifts of calcium IRT lines were found in magnetic Ap stars (Cowley & Hubrig 2005), in several HgMn (Cowley et al. 2007) and blue horizontal branch (BHB) stars in globular clusters (Hubrig et al. 2009). The results of detailed measurement of the exact wavelengths of Ca II infrared lines in the observed stellar spectra give valuable information about anomalous isotopic composition of stellar atmospheres.

Anomalous isotopic composition of quiescent atmospheres of stars can be mainly explained by the presence of light-induced drift (LID). LID was discovered and explained in laboratory experiments by Atutov & Shalagin (1988) and thereafter proposed for study of the chemical anomalies in CP stellar atmospheres by Nasyrov & Shalagin (1993). The theory has been further elaborated and applied successfully for study of anomalous isotope abundances in the HgMn stellar atmospheres by Aret & Sapar (2002) and Sapar et al. (2005, 2008a,b).

We show that Ca isotope anomaly can be explained by the LID effect, using for computations of stellar model atmospheres the code SMART (Sapar & Poolamäe 2003; Aret et al. 2008). SMART enables the computation of evolutionary scenario of diffusive separation of elements and their isotopes in atmospheres of late B- and early A-type stars (Sapar et al. 2008a,b). The software has been updated also for computations of the final equilibrium concentrations of isotopes, assuming the presence of a specific mechanism of generation of the microturbulence due to interaction of photons in the radiative flux with the atomic particles of stellar

plasma. Such an approach enables also to introduce a Reynolds number for stellar atmospheres (Vincent & Lignières 2005).

The study of isotopic anomalies generated by LID demands the precise input data for isotopic and hyperfine splitting in spectral lines of the studied ions. Accurate energy levels, accurate wavelengths, gf values, hyperfine and isotopic splitting are required for computations. However, in spite of numerous laboratory measurements, the isotope and the HFS data are missing for many spectral lines.

Calcium has six stable isotopes with mass numbers 40, 42, 43, 44, 46, 48. Solar abundances of calcium isotopes are ^{40}Ca (96.941%), ^{42}Ca (0.647%), ^{43}Ca (0.135%), ^{44}Ca (2.086%), ^{46}Ca (0.004%) and ^{48}Ca (0.187%) (Anders & Grevesse 1989).

We composed a list of line atomic data for Ca I, Ca II and Ca III lines, which includes in addition to the isotopic shifts also the hyperfine structure shifts for the odd isotope ^{43}Ca . Laboratory shifts for all stable isotopes of IRT lines of Ca II are given by Nörtershäuser et al. (1998b).

Total isotopic shifts of transitions are generally due to the normal mass shift, the specific mass shift and the field (or volume) shift. Field shifts for Ca lines are small and can be neglected. We collected data on the specific mass shift coefficients and the hyperfine structure coefficients from literature. If the necessary data were lacking for specific mass shift coefficients in some levels of calcium atom, then only normal mass shift has been used.

The model calculations have been carried out to obtain final equilibrium concentrations of calcium isotopes in stellar atmosphere using the program SMART. We propose that microturbulence affecting the diffusion is generated by the interaction of photons of the radiative flux with atomic particles of the stellar atmosphere. The obtained Ca line profiles confirm important role of LID in the diffusion of isotopes, which enables to explain the observed anomalous isotopic composition of calcium in the CP stellar atmospheres.

2. ISOTOPIC SHIFTS

Isotopic shifts of spectral lines provide insight into the structure of nuclei and the electric charge cloud around the core. The spectral isotopic shift is the difference between the transition frequency ν_i of two isotopes with masses M and M'

$$IS_i^{MM'} = \nu_i^{M'} - \nu_i^M. \quad (1)$$

Isotopic shift has two causes: isotopic nuclei have different masses and different nuclear charge distribution. The isotopic shift for a given transition in the non-relativistic case is described as a sum of mass and field (volume) shifts (FS) in the following way

$$\delta\nu_i^{MM'} = K_i \frac{M' - M}{MM'} + K_i^{FS} \delta\langle r^2 \rangle, \quad (2)$$

where K_i is the mass shift coefficient of a given transition, M and M' denote the atomic masses of two isotopes, K_i^{FS} is the field shift coefficient and $\delta\langle r^2 \rangle$ is the difference in mean square radii of nuclear charge distribution of the isotopes studied.

The FS in a transition between two levels depends on the distribution of the electric charge density and on the value of $\delta\langle r^2 \rangle$. With increase of nuclear radius r

the atomic levels are shifted higher. The FS grows rapidly with increasing charge number Z , because the nuclei with large Z are larger than with small Z ones, and the electron density in the center is much larger due to stronger electric attraction. Calcium has odd-even staggering dependence of charge radii on neutron number. It is interesting that the calcium isotopes 40 and 48 have almost equal mean square radii of the electric charge. Small values $\delta\langle r^2 \rangle^{40,48}$ are due to the fact that ^{40}Ca and ^{48}Ca are isotopes with doubly magic nuclei in which both neutron and proton shells of both nuclei are closed and spherically symmetric. For Ca lines the isotopic shifts are mainly due to the normal and specific mass shifts, the field shift is negligible.

The mass shift is largest for the lightest elements and it is diminishing with increasing Z . For heavy elements the field shift dominates over the mass shift. The mass shift usually consists of the normal mass shift (NMS) or Bohr mass shift and the specific mass shift (SMS). So we can write mass shift coefficient as $K_i = K_i^{\text{NMS}} + K_i^{\text{SMS}}$. The NMS coefficient at the transition frequency ν_i is given by a simple formula

$$K_i^{\text{NMS}} = -\nu_i \frac{m_e}{M}, \quad (3)$$

where m_e is the electron mass and M is the atomic nuclear mass. The SMS coefficient depends on correlated motion of all electrons and it is determined by the expression

$$K_i^{\text{SMS}} = \sum_{k < j} \frac{\langle \mathbf{p}_k \cdot \mathbf{p}_j \rangle}{h}, \quad (4)$$

where \mathbf{p}_k and \mathbf{p}_j are the moments of electrons. This simple expression demands complicated and detailed quantum-mechanical computations.

The behavior of the specific mass shift is different for various transitions. For example, SMS in the resonant line of Ca I at 423 nm is very small and has opposite sign to the NMS, but in the subordinate line at 732.8 nm it is almost equal to NMS and both are of the same sign. It is known that SMS are usually much larger in transitions with change of the d and f subshell electrons than in the transitions, which involve only s and p subshell electrons (Nörthershäuser et al. 1998a).

We compiled line list incorporating isotopic shifts and the hyperfine splitting of Ca spectral lines. The isotopic transition shifts for Ca I resonance line at 423 nm ($4s^2 \ ^1S_0 - 4s4p \ ^1P_1$) have been determined by several authors (Salumbides et al. 2011; Nörthershäuser et al. 1998b; Andl et al. 1982; Hoekstra et al. 2005), and there is a good agreement between these data. The isotopic shifts and the residual level isotopic shifts for some Ca I transitions and also several level isotopic shift coefficients K^{SMS} are given by Aspect et al. (1991), Weber et al. (1986) and Lorenzen et al. (1983). The transition isotopic shifts in the line at 272 nm, corresponding to the transition ($4s^2 \ ^1S_0 - 4s5p \ ^1P_1$) and hyperfine splitting of higher level of this transition have been measured by Mortensen (2004). For the calcium line at 672 nm, the transition ($4s3d \ ^1D_2 - 4s5p \ ^1P_1$), we used the transition isotopic shifts given by Dammalapati et al. (2010). SMS of this transition is larger than NMS. The isotopic shift and hyperfine structure of ^{43}Ca for the intercombination line at 657.28 nm has been taken from Klingbeil et al. (1979). In the case of Ca II lines there is only one valence electron and therefore the correlation between the valence electrons is zero. Thus, the correlation between the correlated valence electrons and the core is lacking.

Isotopic shifts for the stable isotopes of Ca II, the Fraunhofer spectral lines H ($4s\ ^2S_{1/2} - 4p\ ^2P_{1/2}$) and K ($4s\ ^2S_{1/2} - 4p\ ^2P_{3/2}$), have been measured by several authors (Mårtensson-Pendrill et al. 1992; Maleki & Goble 1992; Lucas et al. 2004), and their results are well consistent.

The structure of low-lying $3D$ levels of Ca II differs from the other levels. So, in the case of Ca II the coefficient of the specific mass shift K_i^{SMS} for the $3D$ levels, describing the correlation between the electronic momenta and the motion of the nucleus, is extremely large, while in contrast the $4S - 4P$ transitions are dominated by K_i^{NMS} .

The transitions from the excited $4p\ ^2P_{1/2,3/2}$ levels to the $3d\ ^2D_{3/2,5/2}$ levels, i.e. the infrared triplet lines (849.8, 854.2, 866.2 nm) for the isotopes of calcium were investigated by Alt et al. (1997), Lucas (2004) and by Nörtershäuser et al. (1998b). Here we use their results.

For the Ca II lines at 645.6 nm and 989.0 nm we took into account only the normal mass shift. For the lines 891.2 nm and 892.7 nm we accepted that the specific mass shift of the upper level $4f\ ^2F$ is equal to zero, but for the level $4d\ ^2D_{3/2,5/2}$ we used SMS shift coefficients given by Kozlov (2004). In the calculation of the SMS value for the transitions $5p\ ^2P_{1/2,3/2} - 6s\ ^2S_{1/2}$ at 985.4 and 993.1 nm, for $6s\ ^2S_{1/2}$ we took the same value of the coefficient K_i as for $5s\ ^2S_{1/2}$.

3. HYPERFINE SPLITTING OF SPECTRAL LINES

Among the stable calcium isotopes only ^{43}Ca has a core with odd number of nucleons, and thus a hyperfine structure of spectral lines. The nuclear spin of ^{43}Ca is $I = 7/2$. If nuclear spin I and the total electron orbital momentum J are larger than $1/2$, then the atomic states are split into hyperfine levels, characterized by total quantum numbers F ($\mathbf{F} = \mathbf{I} + \mathbf{J}$), due to coupling of I and J . Thus, the hyperfine splitting in spectral lines is due to the interaction of electrons with nucleus. This interaction generates the shifts of the individual levels by

$$\delta E = \frac{A}{2}C + \frac{B}{8} \frac{3C(C+1) - 4I(I+1)J(J+1)}{(2I-2)(2J-1)IJ}, \quad I > 1, \quad J > 1/2, \quad (5)$$

where the Casimir factor

$$C = F(F+1) - I(I+1) - J(J+1). \quad (6)$$

The first term accounts for the interaction between the magnetic dipole momentum of the nucleus μ_I and the magnetic field $B_e(0)$, created by electrons at the core center. The magnetic dipole constant A is given by

$$A = \frac{\mu_I B_e(0)}{IJ}, \quad (7)$$

The second term in equation (5) is due to interaction between the electric quadrupole momentum Q and the electric field gradient $\phi_{ij} = \frac{\partial \Phi_j}{\partial x_i}$, produced by electrons. In equation (5) the quantity B is the electric quadrupole coupling constant determined by expression

$$B = e \sum_{ij} Q_{ij} \phi_{ij}. \quad (8)$$

If the quantities A and B are known, then we can determine hyperfine splitting of levels. The quadrupole coupling constant is different from zero, if $I > 1/2$ and $J > 1/2$. The HFS due to electric quadrupole moment Q_s is normally one or two orders of magnitude smaller than that due to the nuclear magnetic moment. In electron transition between the levels with J_l and J_u , the frequency of hyperfine shift is given by

$$\Delta\nu = \frac{A_u C_u - A_l C_l}{2} + \frac{B_u \beta_u - B_l \beta_l}{8}, \quad (9)$$

where we use notation

$$\beta_i = \frac{3C_i(C_i + 1) - 4I(I + 1)J_i(J_i + 1)}{(2I - 2)(2J_i - 1)IJ_i}. \quad (10)$$

Precise analysis of the hyperfine structure requires knowledge of accurate electron wave functions as well as nuclear multipole momenta. To obtain accurate electron wave functions, very often a combined method of configuration interaction (CI) and many-body perturbation theory (MBPT) are applied. The corrections due to core polarization increase the absolute value of all the shift constants. Qualitatively, the core polarization describes the attraction of the valence electrons by the core. This attraction causes enhanced charge density of electrons closer to the nucleus, and also generates larger hyperfine constants. A valence electron polarizes the core and this induced polarization attracts or repels another valence electron.

Values of HFS constants for several CaI levels are given by Grundevik et al. (1979) and Nörtershäuser et al. (1998a). The hyperfine structure constants for levels of the infrared triplet lines of CaII (magnetic dipole coupling constant A and electric quadrupole coupling constant B) and for some other levels of CaII are given in Benhelm (2007), Nörtershäuser (1998b) and Sahoo (2009). We used the measured data of IS and HFS for the infrared triplet lines of CaII given by Nörtershäuser et al. (1998b). HFS constants for H and K line are given also by Selverans et al. (1991) and Goble & Maleki (1990). Review of theoretically calculated and experimentally measured magnetic and electric quadrupole hyperfine structure constants for some states of $^{43}\text{CaII}$ transitions can be found also in Itano (2006), Sahoo(2009) and Mani & Angom (2010). For many levels of CaII we used HFS constants from Safronova & Safronova (2011).

For the fixed values of J and I , the range of F values is $J+I, J+I-1, \dots, |J-I|$. The number of components, into which each fine structure level splits, is $2J+1$ sub-levels if $I > J$, and $2I+1$ if $I < J$.

Using the extrapolation in isoelectronic sequence and simple hydrogenic approximations it is possible to estimate values of A and B . The approximation formulae for isoelectronic sequences were used to overcome the lack of detailed atomic data. Since CaI and ScII belong to the same isoelectronic sequence, then we can make interpolations for some CaI transitions using the data given for ScII, namely the values of A and B for $3d4p\ ^3D_1$ and $3d4p\ ^3F_{2,3,4}$ levels (Avgoulea et al. 2010). The known nuclear momenta of isotope i can be used to estimate the momenta of isotope j of the studied element via the ratios

$$\mu_j = \frac{\mu_i A_j I_j}{A_i I_i}, \quad Q_j = Q_i \frac{B_j}{B_i}. \quad (11)$$

4. RADIATION-DRIVEN DIFFUSION IN TURBULENT ATMOSPHERES

In the present section we discuss the generation of microturbulence in CP stellar atmospheres and isotope separation due to LID in them. The mechanisms of generation of microturbulence in convection-free stellar atmospheres is so far rather enigmatic. According to presently ruling opinion, its physical nature demands 3D modeling of stellar atmosphere, what enables formation of the turbulent atmospheric cell structure. Here we propose to apply the dimensional analysis, somewhat similar to that used in derivation of the Kolmogorov turbulence spectrum.

We start from the usual equation of hydrostatic equilibrium for a plane-parallel stellar atmosphere in the form

$$\frac{dP}{dr} = -\rho(g - a_{\text{rad}}), \quad (12)$$

where a_{rad} is upwards directed effective radiative acceleration and g is the absolute value of downwards directed gravity. Taking into account that the gas pressure $P = NkT$, the mass density $\rho = \sum_i M_i N_i + m_e N_e = \bar{M}N$ and the number density $N = \sum_i N_i + N_e$, we can write

$$\frac{d(NkT)}{dr} = -\bar{M}N(g - a_{\text{rad}}). \quad (13)$$

In stellar atmospheres the thermal gradient is much smaller than the gradient of number density of plasma particles and can be neglected. Thus,

$$\frac{dr}{d \ln N} = -h, \quad (14)$$

where the characteristic height

$$h = \frac{kT}{\bar{M}(g - a_{\text{rad}})} = \frac{1}{\Gamma} \quad (15)$$

and $\Gamma = 1/h$ is the characteristic gradient.

The observed values of the microturbulence velocities can reach the thermal velocities of hydrogen atoms. Generation of such velocities is extremely difficult to understand in the case of lacking convection zones, as it is the case for the quiescent chemically peculiar stellar atmospheres. Such microturbulence velocities would exclude any possibility of diffusive separation of chemical elements. As well known, the atomic diffusion in stellar atmospheres is a slow process and in the stars with solar element abundances, the diffusional effects are canceled by the convection, stellar wind and circular flows due to stellar rotation.

For studies of diffusional stratification it is necessary to specify adequately the microturbulence diffusion coefficient D_t , which is determined by

$$D_t = V_t l_t. \quad (16)$$

Here V_t is the characteristic microturbulence velocity and l_t is the characteristic length of the microturbulence elements. Both of the quantities are hitherto almost

unspecified by strict theoretical analysis, although many prominent scientists have racked their brains on the problem. Here we need only the quantity D_t for analysis of the diffusion of elements and their isotopes.

We assume that radiative flux generates also the microturbulence with velocity V_t . Thus, instead of P we can introduce the quantity

$$P' = \bar{M}N(V^2 + V_t^2)/2, \quad (17)$$

where V is the mean velocity of plasma particles. Introducing also the equivalent temperature T' , which takes into account the microturbulence

$$T' = T(1 + V_t^2/V^2), \quad (18)$$

we can write

$$\Gamma' = \frac{\bar{M}g}{kT'}. \quad (19)$$

Assuming the equality of the characteristic gradients $\Gamma = \Gamma'$, we obtain

$$g - a_{\text{rad}} = \frac{g}{1 + V_t^2/V^2}. \quad (20)$$

From here it follows that the microturbulence velocity

$$V_t = V \left| \frac{a_{\text{rad}}}{g - a_{\text{rad}}} \right|^{1/2}. \quad (21)$$

If $a_{\text{rad}} \ll g$, i.e. far from the Eddington limit, then it holds approximately

$$V_t = V \left(\frac{a_{\text{rad}}}{g} \right)^{1/2}. \quad (22)$$

Using the notation D_i for usual diffusion coefficient of isotope i , we can write the diffusion velocity in the usually accepted form (Michaud 2005):

$$V_i = D_i \left(\frac{M_i(g - a_i)}{kT} + \frac{Z_i M_i g}{2A_i kT} \right) - (D_i + D_t) \frac{d \ln C_i}{dr}, \quad (23)$$

where A_i is the atomic weight of isotope i and C_i is its concentration. In order to take adequately into account different ionization fractions x_j , we summarize over them obtaining the effective acceleration $a_i = \sum_j x_i^j a_i^j$, the effective ionization degree $Z_i = \sum_j x_i^j Z_i^j$ and the effective diffusion coefficient $D_i = \sum_j x_i^j D_i^j$ used in the equation (23).

The first term given in the large brackets in equation (23) accounts for the advection, which depends on D_i and takes into account the gravity g , radiative acceleration a_i and electric field contributions to the acceleration of the isotope, but neglects the thermal diffusion, which gives smaller contribution. In addition there is a purely diffusive term, which includes both the usual atomic diffusion and turbulent diffusion. Further we give a simple expression for D_i and also approximate expression for D_t .

Taking $V_i = 0$ in equation (23) and solving it iteratively relative to the value of radiative acceleration a_i , we obtain the equilibrium concentration profile of the isotope i in a stellar atmosphere.

Let us now introduce the ratio

$$\beta_i = \frac{D_i}{D_i + D_t}. \quad (24)$$

Taking into account that finally must hold $V_i = 0$, we can write for the gradient of the final equilibrium concentration of the isotope i the equation

$$\frac{d \ln C_i}{dr} = \beta_i \left(\frac{M_i(g - a_i)}{kT} + \frac{Z_i M_i g}{2A_i kT} \right). \quad (25)$$

This equation shows that $d \ln C_i / dr$ diminishes, due to the presence of microturbulence, β_i times. Let us now estimate the numeric value of β_i . Approximately the diffusion coefficient (González et al. 1995) for any ion can be written in the form

$$D_i = \frac{V_i}{N_e r_i^2} \varpi_i, \quad r_i = \frac{Z_i e^2}{kT}, \quad (26)$$

where ϖ_i can be treated as a correction factor. This factor for ions has the form

$$\varpi_i = \sqrt{\frac{9(1 + A_i)}{64\pi}} \frac{1}{\ln \Lambda}, \quad \Lambda = \left(\frac{9Z_i}{4\pi N_e r_i^3} + e \right)^{1/2}. \quad (27)$$

The last additive $e = 2.718$ in brackets has been introduced in order to avoid unpleasant negative ϖ_i values at very large electron densities. For the neutral atoms $D_i^0 = 92D_i^1$ (González et al. 1995) holds approximately.

Further, using equations (15) and (14) we replace dr in the left hand of the equation (25):

$$\frac{d \ln C_i}{dr} = -\Gamma \frac{d \ln C_i}{d \ln N}. \quad (28)$$

From equation (25) it follows that in the case of equilibrium holds

$$f_i = \frac{d \ln C_i}{d \ln N} = \frac{\beta_i}{\Gamma} \left(\frac{M_i(g - a_i)}{kT} + \frac{Z_i M_i g}{2A_i kT} \right). \quad (29)$$

This expression for finding the equilibrium gradients of relative concentrations C_i generally does not need many model iteration steps relative to a_i .

Let us now discuss the form of D_t . We suggest that this quantity could be generated by the radiative flux. Similarly to the case of diffusion coefficient, we introduce the kinematic viscosity due to interaction between plasma particles and the radiative flux. We introduce as a necessary characteristic quantity the photon mean path l_t defined by

$$N_a \sigma l_t = 1, \quad (30)$$

where N_a is the total number density of atomic particles and σ is the mean cross section of their interaction with photons of the radiative flux. Here σ is given by

$$\sigma = \frac{1}{N_a} \sum_j \int_{\nu_j}^{\infty} N_j \sigma_j(\nu) d\nu. \quad (31)$$

Our model computations show that a rough value of this mean cross section is $10^{-16} \dots 10^{-18} \text{ cm}^2$ and this value must grow with T_{eff} . We have used this interval of values to estimate the microturbulence kinematic viscosity

$$D_t = V_t l_t. \quad (32)$$

Now we can also introduce the radiative Reynolds number

$$R_r = \frac{D_t}{D_i}. \quad (33)$$

The Reynolds number does not change essentially in the atmospheres of the CP stars, being of the order of $10^3 \dots 10^4$.

Qualitative picture of the isotope stratification does not depend on the value of β_i , while the concentrations of isotopes decrease with decrease of β_i values.

In our previous papers we studied the time-dependent evolution of separation of mercury isotopes due to LID, ignoring presence of microturbulence (Sapar et al. 2008a,b) or accepting a constant value of β_i for all models (Sapar et al. 2009). The presence of microturbulence drastically decelerates the diffusion processes and diminishes the final equilibrium differences of isotope concentrations due to LID.

5. DIFFUSION OF CALCIUM ISOTOPES IN CP STELLAR ATMOSPHERES

As described above, our approach to the generation of the microturbulence is based on two assumptions. First, the velocity of microturbulence V_t in CP stellar atmospheres is determined by the product of the mean thermal velocity and the square root of the ratio a_{rad}/g . The second assumption is that the characteristic length for microturbulence l_t is the free path of photons in the radiative flux. The product of these quantities specifies the diffusion coefficient of microturbulence (Equation 32). Implicitly it has been assumed, that the diffusional phenomena for pure gravity, ignoring the radiative acceleration, are lacking.

Model computations have been carried out using the software SMART for CP stellar atmospheres with gravity $\log g = 4$ and effective temperature T_{eff} values 9000, 10 000, 11 000 and 12 000 K. The isotope abundances at the inner boundary of the model atmosphere were assumed to be the solar ones. The values of the mean impact cross sections σ were taken as constants throughout the atmosphere. The results of computation demonstrated that spectral line profiles are sensitive to the values of σ , but the general picture with dominant role of the heaviest isotope of Ca remains the same. We conclude that the value of σ must be smaller at lower T_{eff} values.

In addition to the computed isotope concentrations, we also obtained column density contributions for each isotope i and the layer l defined by

$$\mu_{il} = C_{il} \mu_{il}^0, \quad (34)$$

which we name the slab densities. Here the quantities μ_{il}^0 are the initial solar slab densities of the isotope i corresponding to the atmospheric layer l .

The column density contributions of the isotopes throughout the model atmosphere are presented in Figures 1–4. The used σ values are given in figure captions. Logarithm of the mean Rosseland optical depths corresponding to model layers covers the interval from -6 to $+2$ with step $1/8$.

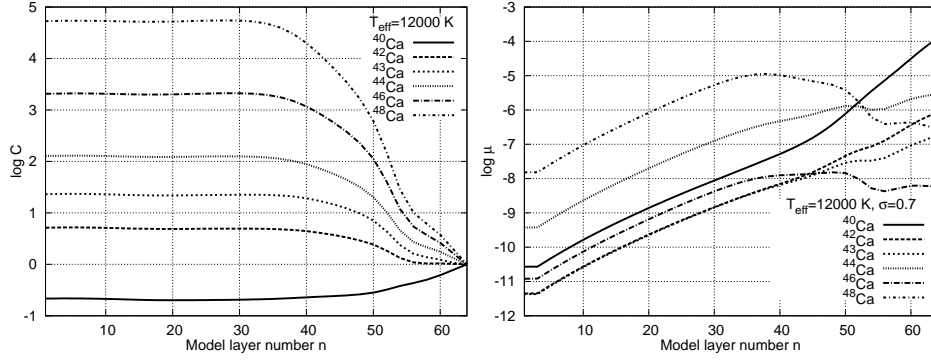


Fig. 1. The Ca isotope concentrations C relative to the solar values (left) and the corresponding isotope slab densities μ (right). The Ca isotope inner boundary concentrations are assumed to be the solar ones. The model parameters are $\log g = 4.0$, $T_{\text{eff}} = 12000 \text{ K}$. The larger is the mass of the isotope, the higher is its concentration. The mean value of the impact cross section is $\sigma = 0.7 \cdot 10^{-16} \text{ cm}^2$.

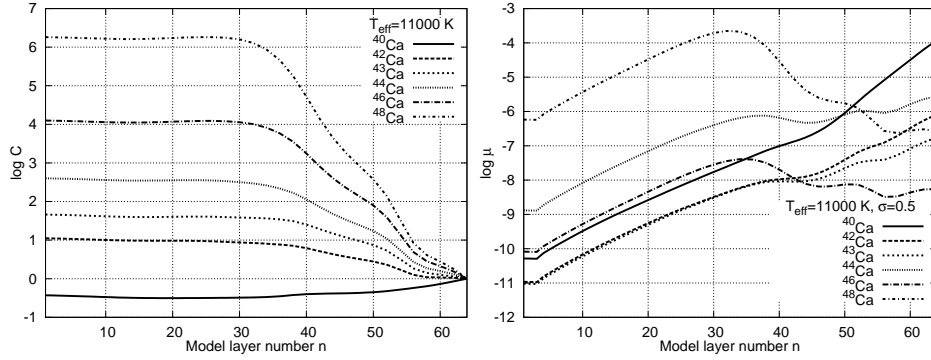


Fig. 2. The same as in Fig. 1, but for $T_{\text{eff}} = 11000 \text{ K}$. The mean value of the impact cross section is $\sigma = 0.5 \cdot 10^{-16} \text{ cm}^2$.

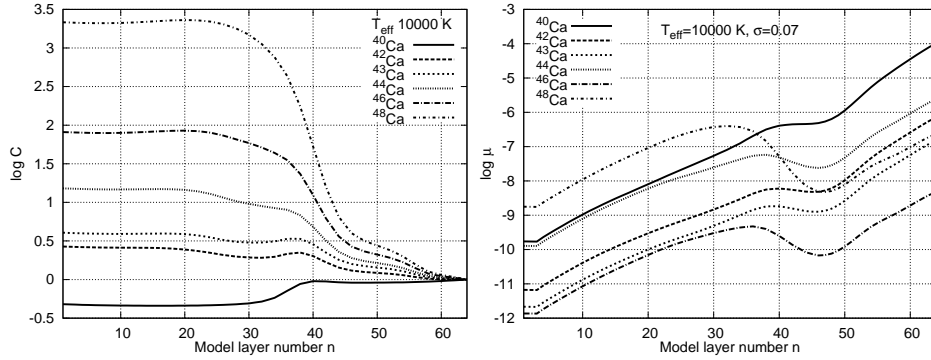


Fig. 3. The same as in Fig. 1, but for $T_{\text{eff}} = 10000 \text{ K}$. The mean value of the impact cross section is $\sigma = 0.07 \cdot 10^{-16} \text{ cm}^2$.

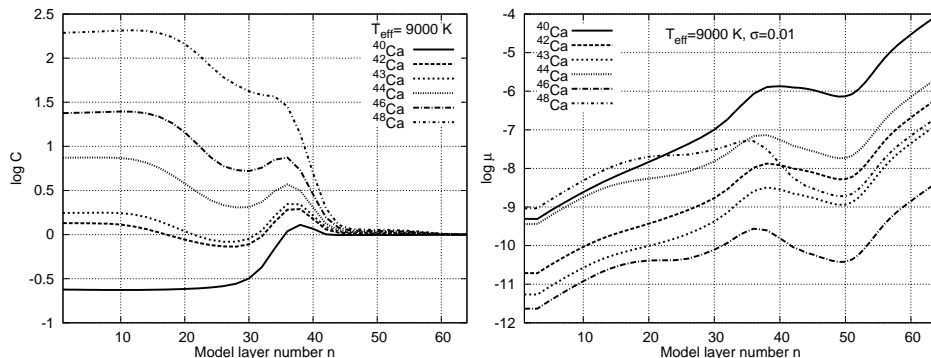


Fig. 4. The same as in Fig. 1, but for $T_{\text{eff}} = 9\,000\text{ K}$. The mean value of the impact cross section is $\sigma = 0.01 \cdot 10^{-16}\text{ cm}^2$.

Figures 5 and 6 show the computed blends of isotopic line profiles of the two components of the Ca II IR triplet at 849.8 and at 866.2 nm. The observed predominance of the ^{48}Ca component increases at higher T_{eff} and larger σ values. These figures demonstrate sensitivity of the computed profiles to the choice of σ values used in Figures 1–4.

We compared two line profiles of Ca II IR triplet components observed by Castelli & Hubrig (2004a) in the spectrum of a HgMn star HD 175640 with the results of our model computations at $T_{\text{eff}} = 12\,000\text{ K}$. In the spectrum of HD 175640 they reported detection of the 0.2 Å redshift of the Ca II IR triplet lines. In figures 7 and 8 we compare the observed and computed profiles of the IR triplet components at 866.2 nm and 849.8 nm, respectively.

We conclude that the LID phenomenon enables to explain the physical mechanism evoking the observed shifts. Diffusional separation of calcium isotopes leads to domination of the heaviest isotope ^{48}Ca in the CP stellar atmosphere. The computed profiles are somewhat wider than the observed ones. This probably means that the input data of isotope splitting should be improved and the depth dependence of the parameter σ should be taken into account in the model computations. In Fig. 9 we demonstrate how different values of σ modify the resulting spectral line profiles.

In the computation of our model two following important factors have been ignored. Isotope ratios at the inner boundary of the atmosphere should be obtained from modeling of physical processes in the sub-atmospheric layers. Also the possible weak stellar wind, which reduces the diffusional stratification phenomena, should be taken into account.

6. CONCLUDING REMARKS

LID has turned out to be hitherto a single physical process capable to generate separation of isotopes of chemical elements. It can be important only in the quiescent stellar atmospheres. Thus, these atmospheres cannot be cool stars with convecting zones, rotating stars with meridional circulation, hot giants with radiation-driven wind, stars with entangled variable magnetic fields and the tidal phenomena in close binaries with different rotation and orbital periods. These dynamical phenomena single out the chemically peculiar main-sequence mercury-

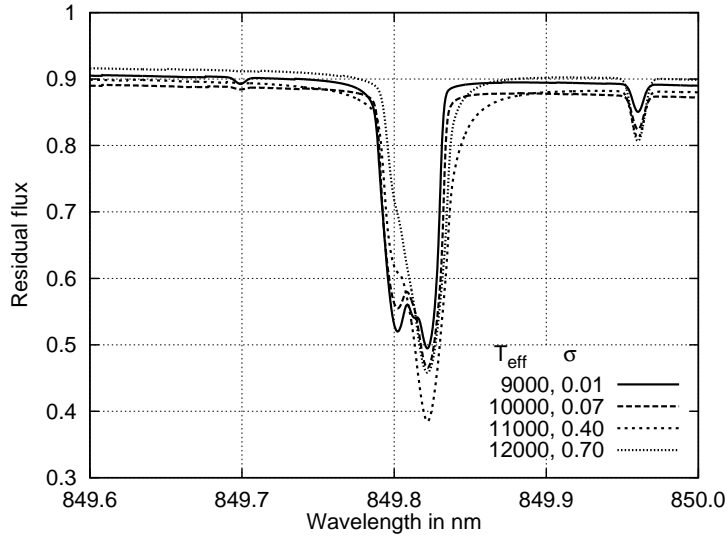


Fig. 5. Residual flux of Ca II IR triplet component at 849.8 nm in the model stellar atmospheres with $\log g = 4.0$ and $T_{\text{eff}} = 9000, 10\,000, 11\,000$ and $12\,000$ K, for different σ values (shown in the insert in the units of 10^{-16} cm^2).

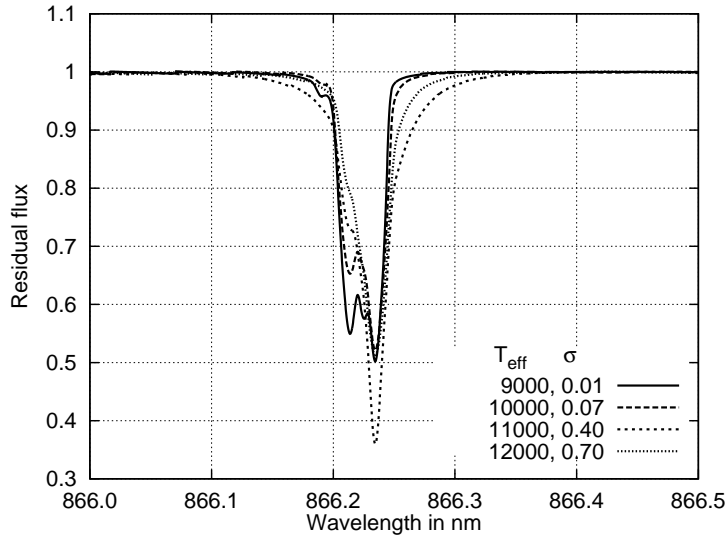


Fig. 6. The same as in Fig. 5, but for the Ca II triplet component at 866.2 nm.

manganese stars of late B and early A spectral classes.

Due to much longer free-flight path of atomic particles in outer layers of stellar atmospheres (comparing to deeper layers), the element diffusion takes place, and in favorite conditions LID can generate weak isotope stratification in some other types of CP stars. Here we report the main papers, in which observations evidently confirm this phenomenon.

The isotopic anomaly and diffusional stratification of calcium in magnetic Ap

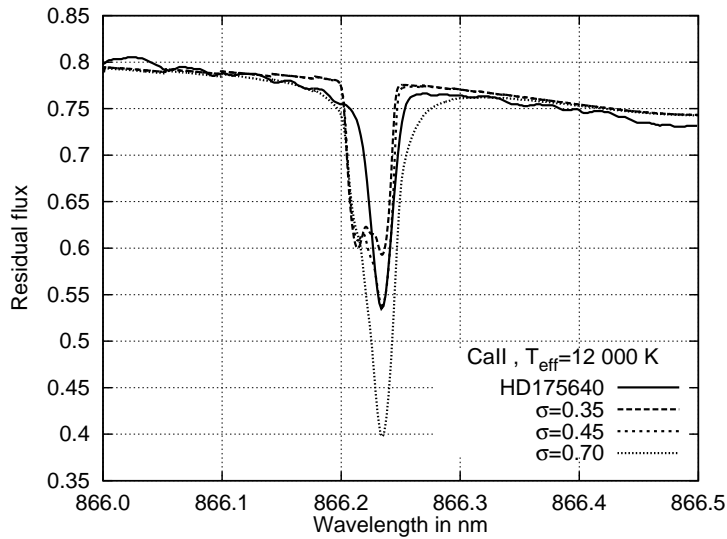


Fig. 7. Comparison of the observed line profile in HD 175640 shifted to 866.23 nm due to predominance of ^{48}Ca with a synthetic profile in the model stellar atmosphere with $\log g = 4.0$ and $T_{\text{eff}}=12\,000$ K. The mean impact cross-sections σ are given in the insert in 10^{-16} cm 2 . A good coincidence of ^{48}Ca line profile for $\sigma = 3.5 \cdot 10^{-17}$ cm 2 shows that the made assumptions are probably quite realistic. However, the abundances of lighter isotopes are higher than observed.

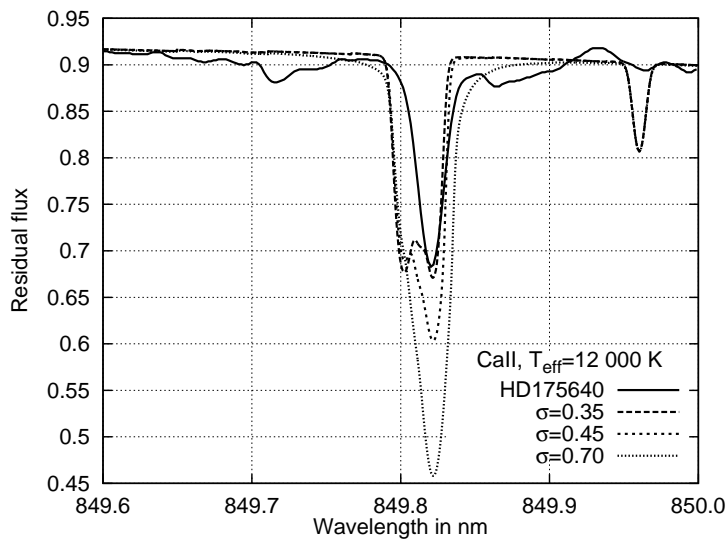


Fig. 8. The same as in Fig. 7, but for the 849.82 nm line.

stars has been found by Ryabchikova et al. (2007, 2008). The isotopic anomalies of He, Hg, Pt, Ca and some other elements in CP stars were studied by Cowley et al. (2008, 2009) and in studies mentioned therein. The isotopes having the longest

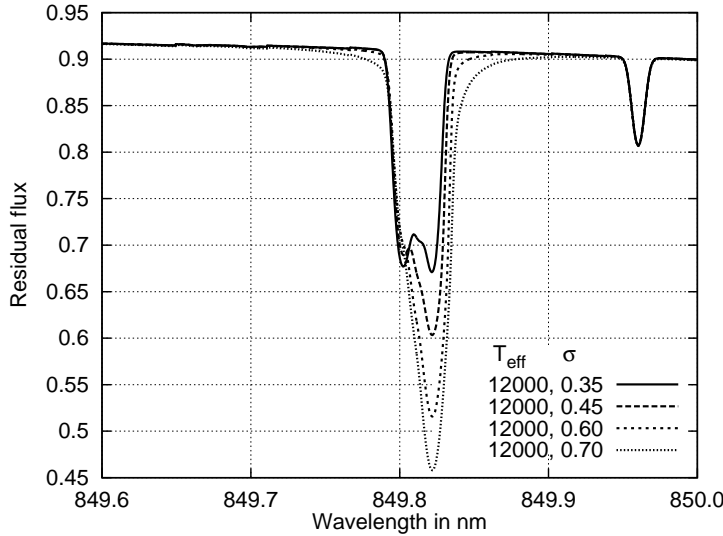


Fig. 9 The same as in Fig. 7, but for the 849.8 nm line. At larger values of σ the role of lighter isotopes on the line profile is less significant.

split wavelength have been detected to be the most overabundant ones, what is an evidence of action of the LID mechanism.

The phenomenon of LID is suppressed by atmospheric velocity fields, including the microturbulence. Landstreet (1988, 1998) and Landstreet et al. (2009) have carried out a study of velocity fields in the main-sequence stars of spectral classes B, A and F, including Ap and rotating stars. Their results can help to determine time-dependency details of the LID phenomenon in the upper layers of moderately non-quietest stellar atmospheres.

This paper is aimed to the study of diffusional separation of Ca isotopes in the atmospheres of hot chemically peculiar HgMn stars due to LID. Microturbulence in the quiescent CP stellar atmosphere is the main factor limiting separation of isotopes. We assumed that the microturbulence velocity V_t is generated by the radiative acceleration and propose a formula to describe it. The collisions between the photons of radiative flux and atomic particles of plasma specify the mean free path of photons l_t which is accepted as the characteristic length of the microturbulence. The microturbulence diffusion coefficient for CP stellar atmospheres was determined according to usual tradition as the product $V_t l_t$. This quantity is used in computations of the isotope stratification due to LID.

The necessary input data file containing parameters of the hyperfine and isotopic splitting of calcium spectral lines has been composed. For adequate computations of radiative transfer in overlapping isotopic spectral lines the spectral resolution was taken extremely high, up to $R = 2.5 \cdot 10^6$. The general picture of Ca isotope stratification turned out to be similar to our previous results obtained for Hg isotopes: an overabundance of the heaviest isotope ^{48}Ca is generated.

Profiles of isotope concentrations in late B and early A spectral type stellar atmospheres are computed assuming that on the inner boundary surface the isotope concentrations have the solar values. The computed Ca infrared triplet line profiles fit well to the observed profiles. We conclude that our suggestions about the

nature of the microturbulence can have realistic physical meaning, which should be analyzed in more details in future.

ACKNOWLEDGMENTS. We are grateful to F. Castelli and S. Hubrig for enabling to use their high-dispersion spectra of the HgMn star HD 175640. This paper was partly supported by the research project SF0060030s08 of the Estonian Ministry of Education and Research.

REFERENCES

- Alt W., Block M., Schmidt V. et al. 1997, *J. Phys. B*, 30, L677
Anders E., Grevesse N. 1989, *Geochim. Cosmochim. Acta*, 53, 197
Andl A., Bekk K., Göring S. et al. 1982, *Phys. Rev. C*, 26, 2194
Aspect A., Bauche J., Godefroid M. et al. 1991, *J. Phys. B*, 24, 4077
Atutov S. N., Shalagin A. M. 1988, *Soviet Astr. Lett.*, 14, 284
Aret A., Sapar A. 2002, *AN*, 323, 21
Aret A., Sapar A., Poolamäe R., Sapar L. 2008, *IAU Symp.*, 252, 41
Avgoulea M., Gangrsky Yu., Marinova K. et al. *J. Phys. G*, 38, 025104
Benhelm J., Kirchmair G., Rapol U. et al. 2007, *Phys. Rev. A*, 75, 032506
Castelli F., Hubrig S. 2004a, *A&A*, 425, 263
Castelli F., Hubrig S. 2004b, *A&A*, 421, L1
Cowley C. R., Hubrig S. 2005, *A&A*, 432, L21
Cowley C. R., Hubrig S., Castelli F. 2008, *Contr. Astr. Obs. Skalnaté Pleso*, 38, 291
Cowley C. R., Hubrig S., Castelli F. et al. 2007, *MNRAS*, 377, 1579
Cowley C. R., Hubrig S., González J. F. 2009, *MNRAS*, 396, 485
Dammalapati U., Norris I., Burrows C. et al. 2010, *Phys. Rev. A*, 81, 023424
Hubrig S., Castelli F., De Silva G. et al. 2009, *A&A*, 499, 865
Hubrig S., North P., Schöller M., Mathys G. 2006, *AN*, 327, 289
Dolk L., Wahlgren G. M., Hubrig S. 2003, *A&A*, 402, 299
Goble A., Maleki S. 1990, *Phys. Rev. A*, 42, 649
González J.-F., LeBlanc F., Artru M.-C., Michaud G. 1995, *A&A*, 297, 223
Grundevik P., Gustavsson M., Lindgren I. et al. 1979, *Phys. Rev. Lett.*, 42, 1528
Hoekstra S., Mollema A. K., Morgenstern R. et al. 2005, *Phys. Rev. A*, 71, 023409
Itano W. M. 2006, *Phys. Rev. A*, 73, 022510
Klingbeil U., Kowalski J., Träger F. et al. 1979, *Z. Physik A*, 290, 143
Kozlov M. G. 2004,
http://www.qchem.pnpi.spb.ru/kozlov/My_papers/notes/2e_sms.pdf
Landstreet J. D. 1988, *ApJ*, 326, 967
Landstreet J. D. 1998, *A&A*, 338, 1041
Landstreet J. D., Kupka F., Ford H. A. et al. 2009, *A&A*, 503, 973
Lorenzen C.-J., Niemax K., Pendrill L. R. 1983, *Phys. Rev. A*, 28, 2051
Lucas D. M., Ramos A., Home J.P. et al. 2004, *Phys. Rev. A*, 69, 012711
Maleki S., Goble A. T. 1992, *Phys. Rev. A*, 45, 524
Mani B. K., Angom D. 2010, *Phys. Rev. A*, 81, 042514

- Michaud G. 1970, ApJ, 160, 641
Michaud G. 2005, EAS Publ. Series, 17, 281
Mårtensson-Pendrill A., Ynnerman A., Warston H. et al. 1992, Phys. Rev. A, 45, 4675
Mortensen A., Lindballe J. J. T., Jensen I.S. et al. 2004, Phys. Rev. A, 69, 042502
Nasyrov K. A., Shalagin A. M. 1993, A&A, 268, 201
Nörtershäuser W., Trautman N., Wendt K., Bushaw B. A. 1998a, Spectrochimica Acta B, 53, 709
Nörtershäuser W., Blaum K., Icker K. et al. 1998b, Eur. Phys. J. D, 2, 33
Preston G. W. 1974, ARA&A, 12, 257
Proffitt C. R., Brage T., Leckrone D. S. et al. 1999, ApJ, 512, 942
Ryabchikova T., Kochukhov O., Bagnulo S. 2007 in *Physics of Magnetic Stars*, 325
Ryabchikova T., Kochukhov O., Bagnulo S. 2008, A&A, 480, 811
Sahoo B. K. 2009, Phys. Rev. A, 80, 012515
Safronova M. S., Safronova U. I. 2011, Phys. Rev. A, 83, 012503
Salumbides E. J., Maslinskas V., Dildar I. M. et al. 2011, Phys. Rev. A, 83, 012502
Sapar A., Poolamäe R. 2003, ASPC, 288, 95
Sapar A., Aret A., Poolamäe R. 2005, EAS Publication ser., 17, 341
Sapar A., Aret A., Sapar L., Poolamäe R. 2008a, Contr. Astr. Obs. Skalnaté Pleso, 38, 273
Sapar A., Aret A., Poolamäe R., Sapar L. 2008b, Contr. Astr. Obs. Skalnaté Pleso, 38, 445
Sapar A., Aret A., Sapar L., Poolamäe R. 2009, New Astr. Reviews, 53, 240
Selverans R. E., Vermeeren L., Neugart R., Lievens P. 1991, Z. Physik D, 18, 351
Vincent A., Lignières F. 2005, EAS Publ. Series, 17, 197
Weber K.-H., Lawrenz J., Niemax K. 1986, Physica Scripta, 34, 14
Wolff S. C., Preston G. W. 1978, ApJS, 37, 371